Identification and Functional Analysis of Circular RNAs in Ankylosing Spondylitis Patient Peripheral Blood Mononuclear Cells

Dan Huang[1], Jian Liu[2], YUAN WANG[3], Lei Wan[3], Yanyan Fang[3], Xiang Ding[3], and Wandong Zhang[4]

[1]The First Affiliated Hospital of Anhui University of Chinese Medicine Department of Pharmacy
[2]Anhui College of Traditional Chinese Medicine
[3]Anhui University of Traditional Chinese Medicine
[4]The First Affiliated Hospital of Anhui University of Traditional Chinese Medicine

January 30, 2024

Abstract

Objectives:To analyze the function and roles of circRNAs in the peripheral blood mononuclear cells (PBMCs) of ankylosing spondylitis (AS) patients. Methods: The expression of AS-related circRNAs were detected by high-throughput RNA-sequencing within the PBMCs of 5 AS cases and healthy controls. After profiling circRNA expression in these samples, differentially expressed circRNAs (DECs) were identified, and a qPCR-based validation approach was used to confirm the differential expression of six of these DECs in patient samples. Spearman's correlation tests and ROC curve analyses were further used to assess the relationship between disease severity and the expression of DECs of interest in AS patients, after which a putative circRNA-microRNAs (miRNAs) interaction network was constructed leading to the detection of six validated DECs with competing endogenous RNA (ceRNA) functionality. Besides, cell experiments were also performed to investigate the potential mechanism of key circRNA in AS. Results: 10,441 circRNAs were identified in these 10 PBMC samples, with 131 total DECs including 89 and 42 that were up- and down-regulated, respectively. In qPCR validation assays, patterns of hsa_circ_0000702, hsa_circ_0006209, hsa_circ_0047920, hsa_circ_0001543, hsa_circ_0072697 and hsa_circ_0005076 were confirmed to align well with RNA-seq results. In addition, the expression levels of hsa_circ_0006209, hsa_circ_0047920, and hsa_circ_0072697 were detected to be positively correlated with disease severity. ROC curve analyses suggested that hsa_circ_0072697 may offer value as a diagnostic biomarker for AS. Cell experiments indicated that hsa_circ_0072697 could suppress the progression of AS by targeting NF-ϰB pathway Conclusions: The identification of six circRNAs with putative ceRNA functionality in AS patients highlights potential molecular mechanisms governing this debilitating disease. However, further research will be necessary to formally confirm the roles of these DECs and their target miRNAs in AS. Further, hsa_circ_0072697 has a good diagnostic value in AS patients, and it could suppress the progression of AS by targeting NF-ϰB pathwa

Identification and Functional Analysis of Circular RNAs in Ankylosing Spondylitis PatientPeripheral Blood Mononuclear Cells

Dan Huang[1,2], Jian Liu[1,2], Yuan Wang[1,2], Lei Wan[1,2], Yanyan Fang[1], Xiang Ding[1], Wandong Zhang[1]

[1]Department of Rheumatology, First Affiliated Hospital of Anhui University of Chinese Medicine, Hefei, Anhui Province, China

[2]Anhui Province Key Laboratory of Modern Chinese Medicine Department of Internal Medicine Application Foundation Research and Development, Hefei, Anhui Province, China

Correspondence to: Jian Liu, Department of Rheumatology, First Affiliated Hospital of Anhui University of Chinese Medicine, 117 meishan road, Hefei, Anhui, 230031, P.R.China

E-mail: *liujianahzy@126.com*

Keywords: Circular RNAs, Ankylosing spondylitis (AS), High-throughput RNA sequencing (RNA-seq), CircRNA-related competing endogenous RNAs (ceRNA)

List of abbreviations

Ankylosing spondylitis AS

Non-coding RNAs ncRNAs

Circular RNAs circRNAs

MiRNA response elements MREs

Competing endogenous RNAs ceRNAs

Systemic lupus erythematosus SLE

Multiple sclerosis MS

Rheumatoid arthritis RA

Primary biliary cholangitis PBC

Osteoarthritis OA

CeRNAs ceRNAs

RNA-sequencing RNA-seq

Peripheral blood mononuclear cells PBMCs

Differentially expressed circRNAs DECs

American College of Rheumatology ACR

Erythrocyte sedimentation rate ESR

C-reactive protein CRP

Bath Ankylosing Spondylitis Disease Activity Index BASDAI

Quality control QC

Receiver operating characteristic ROC

Phosphate-buffered saline PBS

Fetal bovine serum FBS

Enzyme-linked immunosorbent assay ELISA

Horseradish peroxidase HRP

Indirect immunofluorescence IF

Standard deviation SD

Control CN

Area under the curve value AUC

Abstract

Objectives: Circular RNAs (circRNAs) play a diverse range of roles in physiological settings, wherein they can undergo translation, directly interact with RNA-binding proteins, or function by sequestering miRNAs to suppress their functionality. To analyze the function and roles of circRNAs in the peripheral blood mononuclear cells (PBMCs) of ankylosing spondylitis (AS) patients.

Methods: The expression of AS-related circRNAs were detected by high-throughput RNA-sequencing within the PBMCs of 5 AS cases and healthy controls. After profiling circRNA expression in these samples, differentially expressed circRNAs (DECs) were identified, and a qPCR-based validation approach was used to confirm the differential expression of six of these DECs in patient samples. Spearman's correlation tests and ROC curve analyses were further used to assess the relationship between disease severity and the expression of DECs of interest in AS patients, after which a putative circRNA-microRNAs (miRNAs) interaction network was constructed leading to the detection of six validated DECs with competing endogenous RNA (ceRNA) functionality. Besides, cell experiments were also performed to investigate the potential mechanism of key circRNA in AS.

Results: 10,441 circRNAs were identified in these 10 PBMC samples, with 131 total DECs including 89 and 42 that were up- and down-regulated, respectively. In qPCR validation assays, patterns of hsa_circ_0000702, hsa_circ_0006209, hsa_circ_0047920, hsa_circ_0001543, hsa_circ_0072697 and hsa_circ_0005076 were confirmed to align well with RNA-seq results. In addition, the expression levels of hsa_circ_0006209, hsa_circ_0047920, and hsa_circ_0072697 were detected to be positively correlated with disease severity. ROC curve analyses suggested that hsa_circ_0072697 may offer value as a diagnostic biomarker for AS. Cell experiments indicated that hsa_circ_0072697 could suppress the progression of AS by targeting NF-ϰB pathway

Conclusions: The identification of six circRNAs with putative ceRNA functionality in AS patients highlights potential molecular mechanisms governing this debilitating disease. However, further research will be necessary to formally confirm the roles of these DECs and their target miRNAs in AS. Further, hsa_circ_0072697 has a good diagnostic value in AS patients, and it could suppress the progression of AS by targeting NF-ϰB pathway.

Introduction

The ability of immune cells to differentiate between healthy cells and abnormal or non-self entities is critical for efficient elimination of potentially harmful pathogens and cells. However, maintaining self-tolerance while preserving defensive immune responses is a complex process that can be disrupted in certain individuals. This can lead to chronic infections or cancers in immunocompromised individuals or autoimmune diseases in those who fail to maintain immunological tolerance to self-antigens. Over 100 chronic inflammatory or autoimmune diseases have been cataloged, affecting 5-10% of the general population[1]. Ankylosing spondylitis (AS) is the most common arthritic condition affecting the spine, characterized by bone spur formation, back pain, spinal fusion, and disability[2]. AS is driven by disseminated inflammation throughout the skeletal system, which leads to new bone formation that underlies the pathological outcomes observed in AS patients[3].

RNA species play diverse roles in cells, and non-coding RNAs (ncRNAs) with distinct functions have been identified, including circular RNAs (circRNAs)[4, 5]. Although generally classified as ncRNAs, certain circRNAs have been shown to yield polypeptides[6, 7]. CircRNAs often harbor miRNA response elements (MREs) and can function as competing endogenous RNAs (ceRNAs) to suppress miRNA functionality[8, 9]. CircRNAs are crucial regulators of gene expression and have been implicated in a range of pathological processes[10], including cancer, autoimmunity, and diseases of the nervous and cardiovascular systems[11-13]. Autoimmune conditions such as systemic lupus erythematosus (SLE)[14, 15], multiple sclerosis (MS) [16], rheumatoid arthritis (RA)[17, 18], primary biliary cholangitis (PBC)[19], and osteoarthritis (OA)[20, 21] have been shown to be regulated by circRNAs. Thus, to study their specific roles in the context of AS has the potential to yield important insights into the disease's underlying mechanisms and possible therapeutic targets.

The aim of this study was to identify circRNAs that act as ceRNAs (ceRNAs) and play critical functional roles in AS. High-throughput RNA-sequencing (RNA-seq) analyses of peripheral blood mononuclear cells (PBMCs) from AS patients and healthy controls were used to identify differentially expressed circRNAs

(DECs) associated with AS. Together, these findings will provide novel insights into the role of circRNAs in the regulation of AS.

Materials and methods

Patients and controls

Overall, 15 AS patients and 15 healthy age- and sex-matched control patients were recruited for this study from the Department of Rheumatology of the First Affiliated Hospital of Anhui University of Chinese Medicine. These patients had been diagnosed in accordance with the American College of Rheumatology (ACR) modified criteria of New York (1984)[22]without any prior history of cancer, cardiovascular disease, hepatitis, diabetes, or other autoimmune or autoinflammatory diseases. An autoanalyzer (Hitachi 747; Hitachi, Tokyo, Japan) was applied to appraise erythrocyte sedimentation rate (ESR) and high-sensitivity C-reactive protein (CRP) levels in patient blood samples, and a questionnaire was used to compute Bath Ankylosing Spondylitis Disease Activity Index (BASDAI) scores for AS patients. This study had been allowed by the Medical Ethics Committee of the First Affiliated Hospital of Anhui University of Chinese Medicine (2015AH-20), which was consistent with all relevant regulatory guidelines. Prior to the research, all participants were required to provide written informed consent.

PBMC isolation and RNA extraction

Ficoll density gradient centrifugation was used to collect PBMCs from AS and control patient blood samples using room temperature Lymphoprep (Stemcell, USA). Next, a MiRNeasy Mini Kit (Qiagen, Germany) was utilized for extraction of total RNA from these cells which was then purified, quantified, and assessed for quality as discribed in a prior study[23].

High-throughput RNA-seq

RNA library preparation was conducted by a kit of Truseq® chain total RNA sample preparation (Illumina, USA) based on provided directions, with the final library being evaluated with a Qubit 2.0 fluorometer and an Agilent 2100 Bioanalyzer for quantification and quality control. CBOT was then used to dilute the library to 10 pm for cluster generation, after which an Illumina Hiseq 2500 instrument (Illumina) was used for sequencing. All library construction and sequencing were performed by OG-Biotech Inc. (Shanghai, China).

For data analysis, RNA-seq read data were first subjected to quality control (QC) using FastQC (v. 0.11.3) (*http://www.bioinformatics.babraham.ac.uk/projects/fastqc*), after which low-quality reads, rRNA sequences, and adapter sequences were trimmed with the seqtk tool (*https://github.com/lh3/seqtk*). Mapping to the hg38 human reference genome was then performed with the BWA-MEM computer program (v 2.0.4), circRNAs were estimated by utilizing CIRI (33), while SRPBM was used to determine circRNA counts(34). Screening for circRNAs that were differentially expressed in AS and control samples was conducted utilizing edgeR using the following criteria: FC [?] 2 or < 0.5 and P -value < 0.05. Functional characterization of circRNAs of interest was performed through GO and KEGG enrichment analyses of the parental genes from which these circRNAs were derived. The miRNA targets of these DECs were predicted with the miRanda software-based custom-built software application used by OG-Biotech(35), and Cytoscape was used for circRNA-miRNA network visualization(36).

RT-qPCR

To validate the results of RNA-seq analyses, cDNA was prepared from 15 samples from AS patients and control donors via reverse transcription. The levels of three up-regulated and three down-regulated DECs were then assessed in these samples via qPCR using the Universal SYBR Green Master Mix. The primers that had been designed and synthesized by OG-Biotech Inc. (Table 1). Relative circRNA expression was assessed via the 2^{-Cq} approach, and receiver operating characteristic (ROC) curve analyses were used to differentiate between samples in the control and AS patient groups.

Table1: Specifific circRNAs primers used for qRT-PCR analysis

gene	primers sequences	pcr product length(bp)
GAPDH	F: ACAACTTTGGTATCGTGGAAGG	101
	R: GCCATCACGCCACAGTTTC	
hsa_circ_0000702	F: TGCTTCGTGTGAGAATGCTG	191
	R: CAAACTGGCTCGGTCAAACA	
hsa_circ_0006209	F: GAAGATCGCCAAGCTGTACG	166
	R: TACTCTGCAACTGGGTGAGG	
hsa_circ_0047920	F: TACCCTCTTTGTGGCTGGAG	164
	R:TACCCTCTTTGTGGCTGGAG	
hsa_circ_0072697	F: GCTTATCCAACCAGCGTATGT	181
	R: TACATGGATGCACTGGGGAG	
hsa_circ_0001543	F:ACTCTGAACTTCCCTGGTCG	139
	R: TCACATCTCCCCTCTCCTGA	
hsa_circ_0005076	F: CAGTCAGCAGCACAACAGAG	158
	R: TCCAGCAGCACTAGGAAACA	

Cell culture

PBMCs were obtained from human peripheral blood using Ficoll-Paque PLUS (GE Healthcare, Sweden) density gradient centrifugation. Briefly, whole blood was diluted with equal volume of phosphate-buffered saline (PBS) and layered on top of Ficoll-Paque PLUS. After centrifugation, the PBMC layer was collected and washed twice with PBS. The cells were then resuspended in RPMI Medium Modified (Thermo Fisher Scientific, USA) supplemented with 10% heat-inactivated fetal bovine serum (FBS) (Thermo Fisher Scientific, USA) and 1% penicillin/streptomycin (Thermo Fisher Scientific, USA). PBMCs were cultured in a humidified incubator at 37°C with 5% CO_2.

Cell proliferation assay

Cells were seeded into 96-well plates at a density of 5×10^3 cells per well and incubated at 37°C in a humidified atmosphere containing 5% CO_2. After 24 hours of incubation, the cells were treated with different concentrations of test compounds for various time periods. At the end of the treatment, the medium was removed, and 100 μL of fresh medium containing 10 μL of CCK-8 solution (BA00208, BIOSS) was added to each well. The plates were then incubated for an additional 2 hours at 37°C. The absorbance was measured at 450 nm using a microplate reader (BioTek, USA).

Cell cycle analysis by flow cytometry

First, we washed cells with cold PBS, then trypsinized. The cells were then centrifuged at 2000 rpm for 5 min, and the supernatant was carefully aspirated leaving approximately 50 μL of residual solution. Cells were then resuspended in cold PBS and washed twice. The cell pellet was resuspended in 1 mL of pre-cooled ethanol and fixed at 4 °C for at least 2 h or overnight. After fixation, the cells were centrifuged and the supernatant was removed. Fixed cells were washed twice with pre-cooled PBS and resuspended in 0.5 mL of RI/RNase staining buffer (550825, BD Biosciences, USA) for 15 min at room temperature in the dark. Stained cells were then analyzed using a flow cytometer (CytoFLEX, BECKMAN) equipped with appropriate lasers and filters.

Cell apoptosis assay by flow cytometry

In this study, we used flow cytometry to analyze cell apoptosis. Cells were harvested by centrifugation after digestion and washed with cold PBS. They were collected (including cells from culture supernatant) and resuspended in 500 μL of Binding Buffer. Next, we added 5 μL of Annexin V-FITC (AP101, Biotech) and 10 μL of propidium iodide (PI) to each sample, gently vortexed samples, then incubated for 5 mins at room temperature in the dark. Stained cells were then analyzed using a flow cytometer (CytoFLEX, BECKMAN) equipped with appropriate lasers and filters.

Enzyme-linked immunosorbent assay (ELISA)

ELISA was used to measure the concentration of the target protein. Briefly, 96-well plates were coated with capture antibody and left overnight at 4°C. Plates were then washed with PBST and blocked with 3% BSA solution for 1 hour at room temperature. Plates were washed again and samples, standards and controls were added to the wells. After 2 hours of incubation at room temperature, the plates were washed again and detection antibodies were added. After incubation with the detection antibody for 1 h at room temperature, the plate was washed and then treated with substrate solution (Wuhan jiyinmei Biotechnology Co., Ltd) for 20 min. Finally, the stop solution was added and the absorbance at 450 nm was measured using a microplate reader (Redu). The concentration of the target protein in the sample was determined by comparing the absorbance of the sample to a standard curve. All experiments were performed in triplicate.

Western blot analysis

For Western blot analysis, cell samples were harvested and lysed by adding 600 μl of RIPA Cell Lysis Buffer (P0013B, Beyotime) containing 0.6 mM PMSF. The lysate was centrifuged at 12,000 rpm for 15 min at 4°C and the supernatant was collected. We added 5X SDS-PAGE protein loading buffer to the collected protein samples at a ratio of 1:4. Heat in a boiling water bath for 15 minutes to fully denature the protein. After the sample was cooled to room temperature, we loaded the protein sample directly into the sample well of the SDS-PAGE gel, and added 5-10ul to each well, and kept constant voltage 80v electrophoresis for 1 hour. Equal amounts of proteins were separated by SDS-PAGE and transferred to PVDF membranes (Millipore). After blocking with 5% skim milk, the membrane was incubated with the primary antibody overnight at 4°C, followed by a horseradish peroxidase (HRP)-conjugated secondary antibody for 2 hours at room temperature. The protein bands were visualized using the ECL Ultra Sensitive Luminescence Kit (340958, Thermo), and the analysis of the film bands was performed using Image J software.

Indirect immunofluorescence

Indirect immunofluorescence (IF) is a common method for detecting protein expression and localization in cells. In this study, the cell suspension was first centrifuged at 2800 rpm, 4°C for 5 min, the supernatant was discarded, and fixed with 2 ml of 4% paraformaldehyde (Sigma-Aldrich) for 10 min at room temperature. Cells were then incubated with 0.5% Triton X-100 (Sigma-Aldrich) in PBS for 30 min. We removed 0.5% TritonX-100, washed with PBS-T, added goat serum blocking solution dropwise, and incubated in a 37°C incubator for 30min. After blocking, we directly suck out the goat serum blocking solution without washing. Then, enough primary antibody (p-IKBα, 1:300, bs-5515R, Bioss; p-NF-ϰB, 1:100, BS4135, Bioworld) was added dropwise, covered, and incubated in a 37°C incubator for 1 hour. The primary antibody was removed, and enough immunofluorescent secondary antibody (goat anti-rabbit IgG (FITC) 1:400) was dropped, for 30 minutes in the dark at 37°C. Finally, we mounted the slides with anti-fade mounting medium (containing DAPI). Fluorescent sections were scanned using a digital slide scanner (Pannoramic MIDI).

Statistical analysis

GraphPad Prism v6 was utilized for ROC curve and correlation analyses, as well as the evaluation of relative circRNA expression. Student's t-tests and Spearman rank correlation analyses were used to compare the data, and the results are presented as means ± standard deviation (SD). A P -value < 0.05 was the threshold of significance for the current research.

Results

Patient characteristics

There were no considerable discrepancies between the AS and control groups with respect to sex or age distributions (Table 2).

Table 2 Clinical characteristics of study population

Indexes	AS	Control	P value

Sex (M/F)	11/4	11/4	1.00
Age (years)	33.60±8.24	34.60±7.03	0.723
ESR(mm/h)	51.27±25.50	NA	NA
CRP(mg/dL)	55.30±35.31	NA	NA
BASDAI(score)	6.55±0.48	NA	NA

Detection of circRNA expression patterns in the PBMCs of AS and control groups

Using a CIRI-based computational pipeline, circRNAs present in RNA-seq data derived from the PBMCs of AS and control (CN) groups were predicted. In total, 10,441 distinct candidate circRNAs were detected in analyzed samples, of which 5,917 (56.7%) were known and 4,524 (43.3%) were novel in human samples. Overall, 3,432 circRNAs were present only in the AS group, 2,562 only in the CN group, and 4,447 present in both groups (Fig. 1A). Of these 10,441 circRNAs, 883 (8.46%) were derived from introns, 9,303 (89.1%) were generated from exonic sequences, and the remaining 255 (2.44%) were derived from intergenic regions. 10,186 different circRNAs originating from 3,968 parental genes were detected in these PBMCs samples, with 1,920 (48.4%) and 2,048 (51.4%) of the parental protein-coding genes producing one and more than one circRNA, respectively. A single gene encoding a phosphatidylinositol binding clathrin assembly protein was found to be the source of 32 different circRNAs in these samples (Fig. 1B). These circRNAs exhibited a chromosomal distribution pattern that was roughly consistent with chromosome size, and chromosomes 1, 2, and 3 produced the most circRNAs in these analyzed samples (Fig. 1C).

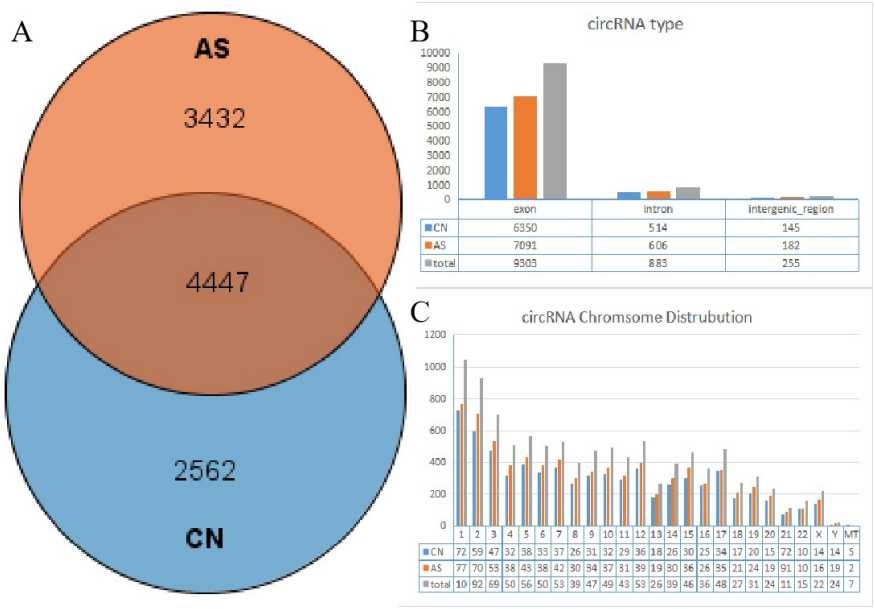

Figure 1. Bioinformatics analysis of circRNAs in PBMC with AS.

(A)The landscape of circRNAs in the AS and control groups.

(B) Bar diagram showing the different categories of circRNAs.

(C) Bar diagram showing the distribution of circRNAs in human chromosomes. CircRNA categories were investigated in Control & AS, Control, and AS groups. Most of the circRNAs originated from exons; some from introns, and a few from intergenic region sources.

Identification of differentially-expressed circRNAs associated with AS

The edgeR tool was next used to identify DECs by comparing the relative circRNA expression levels in the AS and CN groups with the following threshold criteria: FC [?] 2 or [?] 0.5, P -value < 0.05. Volcano plots (Fig. 2A), scatter plots (Fig. 2B), and hierarchical clustering analyses (Fig. 2C) were then used to highlight the patterns of DEC expression in these two groups. By this method, 131 DECs were identified, including 89 up-regulated and 42 down-regulated DECs, in AS and control groups. The top 10 up-and down-regulated DECs in the AS group were compiled in Table 3.

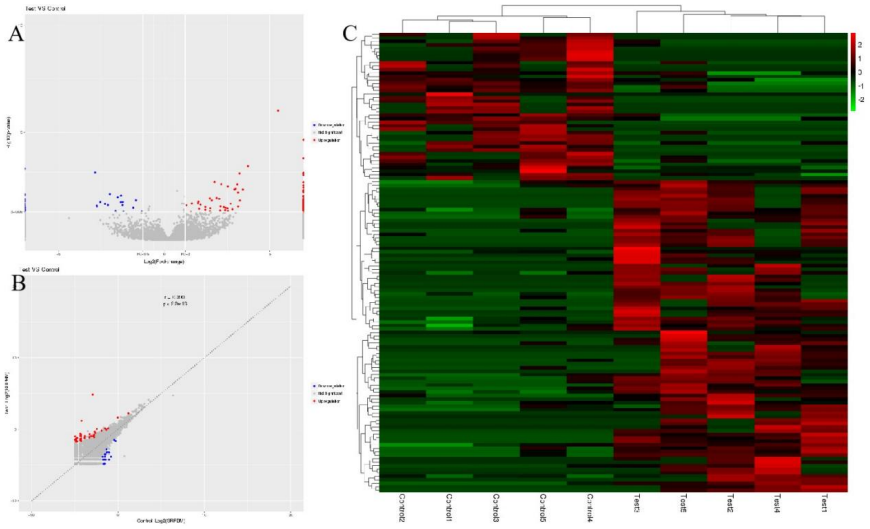

Figure 2. Sequences determining the circRNAs expression profifiles in five AS patients and five healthy controls.

Volcano plot (A), Scatter plot (B) and Hierarchical clustering (C) showing differentially expressed circRNAs in the AS group compared to the control group. The green and blue colors indicate >2 fold reduced levels of expression of the dysregulated circRNAs in the AS group compared to the control group in the hierarchical clustering and volcano plot analyses, respectively (P <0.05). Red color indicates >2 fold increased expression of dysregulated circRNAs in the AS group compared to the control group (P <0.05).

Table 3 Top10 known DECs which were up-regulated and down-regulated with expressed in both AS and the control groups

known_circRNA	locus	circRNA_type	gene_id	log2FC	Pvalue	updown
hsa_circ_0001543	5:143399656|143400852(-)	exon	NR3C1	-3.277014644	0.000738814	DOWN
hsa_circ_0072697	5:65567513|65572286(+)	exon	PPWD1	-3.191813468	0.025746356	DOWN
hsa_circ_0005076	21:34102835|34125480(+)	exon	MRPS6	-3.178812202	0.027278402	DOWN
hsa_circ_0002174	3:195959183|195960086(-)	intergenic_region	n/a	-3.021206039	0.017090038	DOWN
hsa_circ_0088377	9:122855184|122859102(-)	exon	RC3H2	-2.667614456	0.023374156	DOWN
hsa_circ_0006887	6:129611533|129618852(-)	exon	ARHGAP18	-2.309377197	0.045317978	DOWN
hsa_circ_0051220	19:41378281|41378519(+)	exon	AC011462.1	-2.040800493	0.008653912	DOWN
hsa_circ_0004479	12:120782655|120791557(-)	exon	SPPL3	-1.971124173	0.023798904	DOWN
hsa_circ_0039353	16:53155926|53157541(+)	exon	CHD9	-1.960905319	0.017185637	DOWN
hsa_circ_0005044	11:36393846|36403378(+)	exon	PRR5L	-1.930379859	0.047493127	DOWN
hsa_circ_0001565	5:179709873|179716294(+)	exon	CANX	2.992894697	0.033680084	UP
hsa_circ_0005584	18:54159765|54205157(-)	exon	MBD2	3.020913732	0.003215588	UP
hsa_circ_0043403	17:39264175|39265453(-)	exon	FBXL20	3.145629067	0.020659935	UP
hsa_circ_0005594	7:139266333|139272440(+)	exon	UBN2	3.240528454	0.037288142	UP

hsa_circ_0008624	2:175979810|175995646(-)	exon	LNPK	3.331371915	0.004423213	UP
hsa_circ_0058051	2:214767482|214797117(-)	exon	BARD1	3.494312623	0.006275454	UP
hsa_circ_0004906	19:37425868|37426378(-)	exon	ZNF569	3.496233783	0.027657039	UP
hsa_circ_0000702	16:53254438|53274302(+)	exon	CHD9	3.579365962	0.014726482	UP
hsa_circ_0006209	18:79695225|79704917(+)	exon	CTDP1	3.720906049	0.004552572	UP
hsa_circ_0047920	18:69873144|69896045(-)	exon	CD226	3.96948724	0.000375734	UP

Functional enrichment analyses on the parental genes of DECs

Both circRNAs and mRNAs are derived from shared pre-mRNA precursors, so we next explored the functional roles of the parental genes sequences from which these DECs were derived using the ClusterProfiler tool to conduct GO and KEGG enrichment analyses for the 127 DECs (four intergenic circRNAs had been excluded from this analysis).

The top 30 GO terms enriched by these DECs were compiled in Figure 3A. Significant biological process terms included B cell homeostasis (GO:0001782), lymphocyte homeostasis (GO:0002260), leukocyte homeostasis (GO:0001776), RNA phosphodiester bond hydrolysis, endonucleolytic (GO:0090502), homeostasis of number of cells (GO:0048872), small GTPase mediated signal transduction (GO:0007264), positive regulation of GTPase activity (GO:0043547), antigen receptor-mediated signaling pathway (GO:0050851), sister chromatid cohesion (GO:0007062), B cell receptor signaling pathway (GO:0050853), covalent chromatin modification (GO:0016569), regulation of small GTPase mediated signal transduction (GO:0051056), regulation of GTPase activity (GO:0043087), RNA phosphodiester bond hydrolysis (GO:0090501), chromosome organization (GO:0051276), chromosome segregation (GO:0007059), nucleocytoplasmic transport (GO:0006913), nuclear transport (GO:0051169), chromatin organization (GO:0006325), and protein polymerization (GO:0051258). Top enriched cellular component terms included Golgi-associated vesicle membrane (GO:0030660), Golgi-associated vesicle (GO:0005798), nuclear speck (GO:0016607), nuclear body (GO:0016604), lytic vacuole (GO:0000323), lysosome (GO:0005764), cytosol (GO:0005829), chromatin (GO:0000785), vacuole (GO:0005773), lysosomal membrane (GO:0005765), spindle (GO:0005819), intracellular membrane-bounded organelle (GO:0043231), nucleoplasm (GO:0005654), vacuolar membrane (GO:0005774), cytoplasm (GO:0005737), intracellular ribonucleoprotein complex (GO:0030529), ribonucleoprotein complex (GO:1990904), intracellular organelle (GO:0043229), and cytoplasmic region (GO:0099568). Moreover, top molecular function terms included GTPase activator activity (GO:0005096), endoribonuclease activity (GO:0004521), GTPase regulator activity (GO:0030695), organic cyclic compound binding (GO:0097159), ribonuclease activity (GO:0004540), RNA binding (GO:0003723), enzyme activator activity (GO:0008047), ubiquitin-protein transferase activity (GO:0004842), ubiquitin-like protein transferase activity (GO:0019787), endonuclease activity (GO:0004519), Ras GTPase binding (GO:0017016), Rab GTPase binding (GO:0017137), nucleic acid binding (GO:0003676), small GTPase binding (GO:0031267), enzyme regulator activity (GO:0030234), kinase binding (GO:0019900), molecular function regulator (GO:0098772), GTPase binding (GO:0051020), protein serine/threonine kinase activity (GO:0004674), protein kinase activity (GO:0004672), tubulin binding (GO:0015631), purine ribonucleoside triphosphate binding (GO:0035639), cytoskeletal protein binding (GO:0008092), nuclease activity (GO:0004518), and transferase activity (GO:0016740).

KEGG enrichment analysis was conducted and led to the identification of 143 pathway terms, 44 of which were found to be significantly enriched by these DEC parental genes (P <0.05). The top 30 enriched pathways were compiled in Fig. 3B, mainly including the ErbB signaling (hsa04012), Phospholipase D signaling (hsa04072), Gap junction (hsa04540), GnRH signaling (hsa04912), Choline metabolism in cancer (hsa05231), Endocrine and other factor-regulated calcium reabsorption (hsa04961), T cell receptor signaling (hsa04660), B cell receptor signaling (hsa04662), Thyroid hormone synthesis (hsa04918), Gastric acid secretion (hsa04971), Bacterial invasion of epithelial cells (hsa05100), Chronic myeloid leukemia (hsa05220), mTOR signaling (hsa04150), Ras signaling (hsa04014), EGFR tyrosine kinase inhibitor resistance (hsa01521), and Oxytocin signaling (hsa04921) pathways.

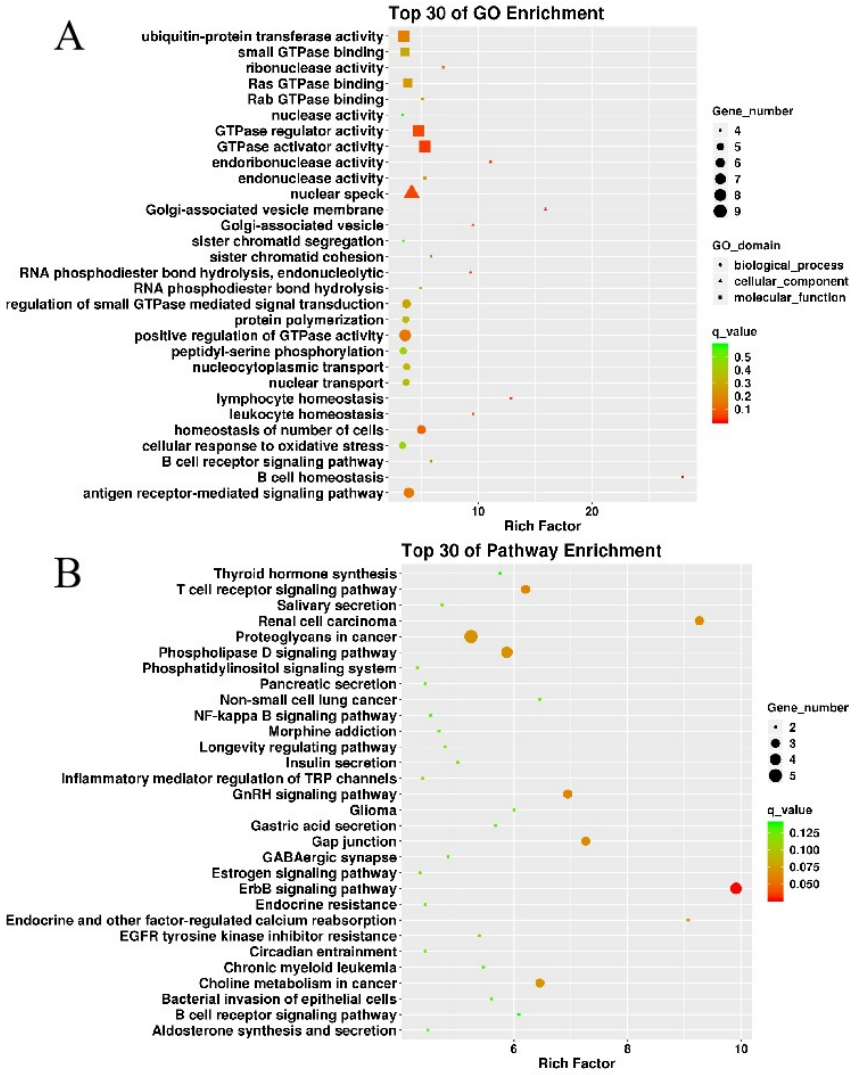

Figure 3. Results of Gene Ontology and KEGG pathway enrichment analysis for the parental genes of DECs.

Top 30 classes of GO enrichment terms.

Top 30 classes of KEGG pathway enrichment terms.

RT-qPCR-based validation of RNA-seq results

To verify the validity of the RNA-seq data generated above, six DECs were selected for RT-qPCR-based validation in a larger cohort of PBMC samples. The observed patterns of differential circRNA expression in AS and control samples were confirmed by these analyses. Specifically, hsa_circ_0000702, hsa_circ_0006209, and hsa_circ_0047920 were found to be considerably upregulated, while hsa_circ_0001543, hsa_circ_0072697, and hsa_circ_0005076 were significantly downregulated (Fig. 4). These RNA-seq results were deemed stable and reliable. As such, these RNA-seq results were deemed stable and reliable.

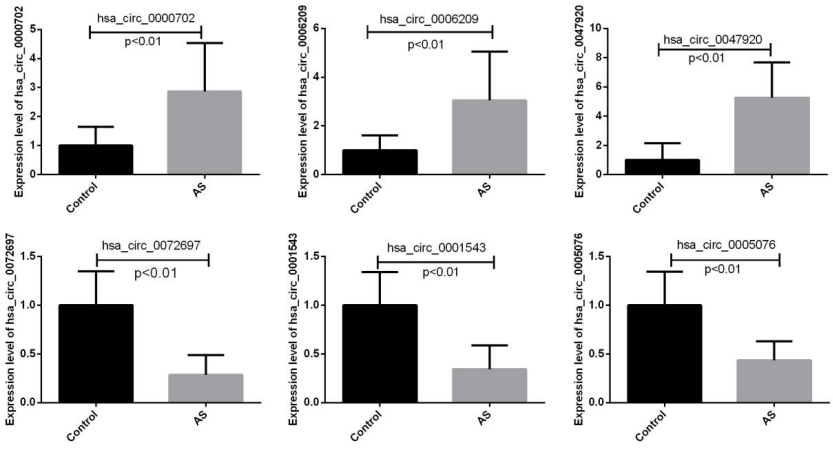

Figure 4. Verification of differentially expressed circRNAs (DECs) by qRT-PCR.

The expression of 6 circRNAs in PBMC was detected by qRT-PCR; y-axis shows as expression fold changes.

Assessment of the correlation between circRNA expression and AS-related clinical findings

To assess whether the six RT-qPCR-validated DECs (hsa_circ_0000702, hsa_circ_0006209, hsa_circ_0047920, hsa_circ_0001543, hsa_circ_0072697, hsa_circ_0005076) could be relevant biomarkers of AS disease, we conducted a series of ROC curve and correlational analyses. The expression of hsa_circ_0006209 and hsa_circ_0047920 was detected to be positively correlated with AS patient CRP levels (Fig. 5A and 5B), while hsa_circ_0072697 levels were negatively correlated with ESR and BASDAI levels in these patients (Fig. 5C and 5D). ROC curve analyses indicated that all six DECs were able to effectively differentiate between AS and control PBMC samples, and hsa_circ_0072697 exhibited the highest area under the curve value (AUC: 0.9867; 95% confidence interval [CI]: 0.9552-1.018;P <0:0001). Therefore, hsa_circ_0072697 may be a particularly promising diagnostic biomarker for AS (Fig. 6, Table 4).

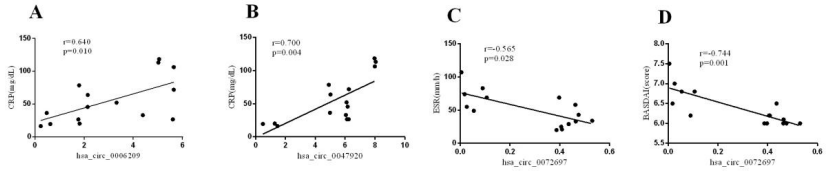

Figure 5. Correlation between circRNAs and clinical disease activities.

(A) There was close positive correlation of the hsa_circ_0006209 levels with CRP levels in AS.

(B) There was close positive correlation of the hsa_circ_0047920 levels with CRP levels in AS.

(C-D) There was close negative correlation of the hsa_circ_0072697 levels with ESR and BASDAI levels in AS.

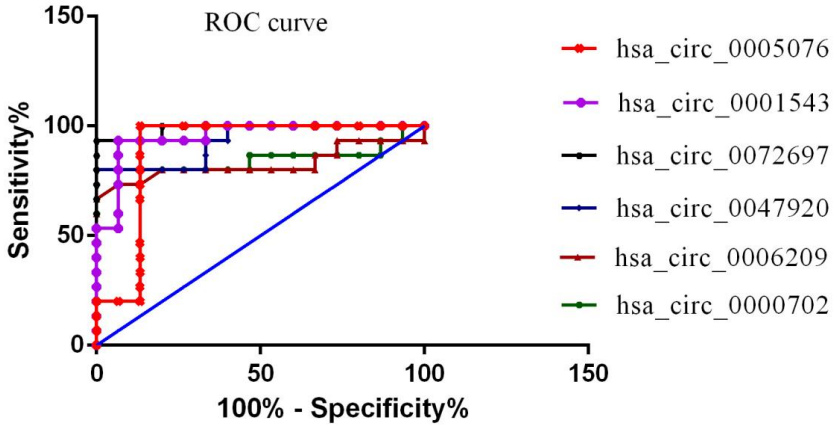

Figure 6. The visualization of the ROC curve.

Table 4. Detals of the ROC curve

	Area	Std. Error	95% confidence interval	P value
hsa_circ_0000702	0.8489	0.08357	0.6851 to 1.013	0.0011
hsa_circ_0006209	0.8267	0.08631	0.6575 to 0.9959	0.0023
hsa_circ_0047920	0.9289	0.04580	0.8391 to 1.019	<0.0001
hsa_circ_0072697	0.9867	0.01605	0.9552 to 1.018	<0.0001
hsa_circ_0001543	0.9511	0.03818	0.8763 to 1.026	<0.0001
hsa_circ_0005076	0.8933	0.07213	0.7519 to 1.035	0.0002

Predictive identification of DECs with potential ceRNA functionality

Many prior investigations have illuminated the ability of specific circRNAs to function as ceRNAs, binding to miRNAs in a sequence-specific behavior and thereby inhibiting their expression or function. As such, we next predicted the potential miRNA targets of identified DECs using miRanda-based customized software developed by OG-Biotech based upon known sequence complementarity between DECs and miRNAs, which then facilitated the construction of a circRNA network incorporating 87 DECs and their putative target miRNAs (Fig. 7). The majority of circRNAs in this network were predicted to interact with more than 10 miRNAs, while hsa_circ_0015733 was predicted to bind to 10 miRNAs. Notably, hsa_circ_0005076, hsa_circ_0005044, hsa_circ_0008699, hsa_circ_0007120, hsa_circ_0062021, hsa_circ_0000699, hsa_circ_0002520, hsa_circ_0009130, hsa_circ_0004617, hsa_circ_0061782, hsa_circ_0056567, hsa_circ_0040827, and hsa_circ_0008410 were predicted to harbor binding sites for hundreds of different miRNAs.

The potency of a given ceRNA interaction is dependent upon the number of miRNAs, with circRNAs and miRNAs competing for target binding in a complex intracellular environment. To identify potential circRNA-miRNA-mRNA regulatory networks, we utilized the miRTarBase database in conjunction with Functional MTI analysis. Cytoscape software was used to generate six circRNA-miRNA-mRNA networks for the RT-qPCR-validated circRNAs (Fig. 8).

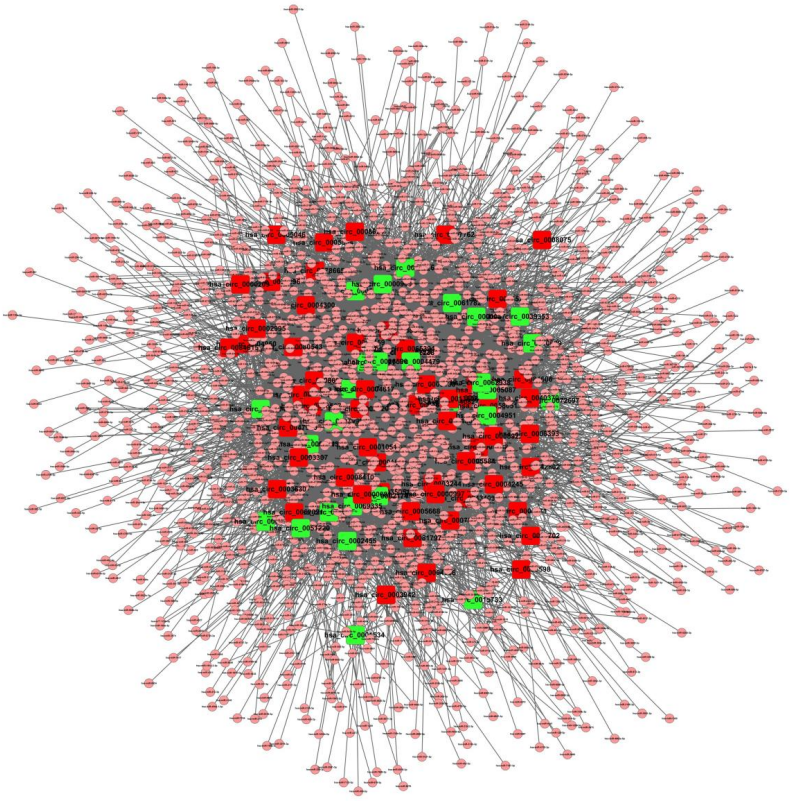

Figure 7. The constructed circRNA-miRNA network.

This network was based on expression profile results and was created by specialized software. Dysregulated circRNAs (green and red nodes) with the highest magnitude of change, were predicted to be functionally connected with their targeted miRNAs in the network.

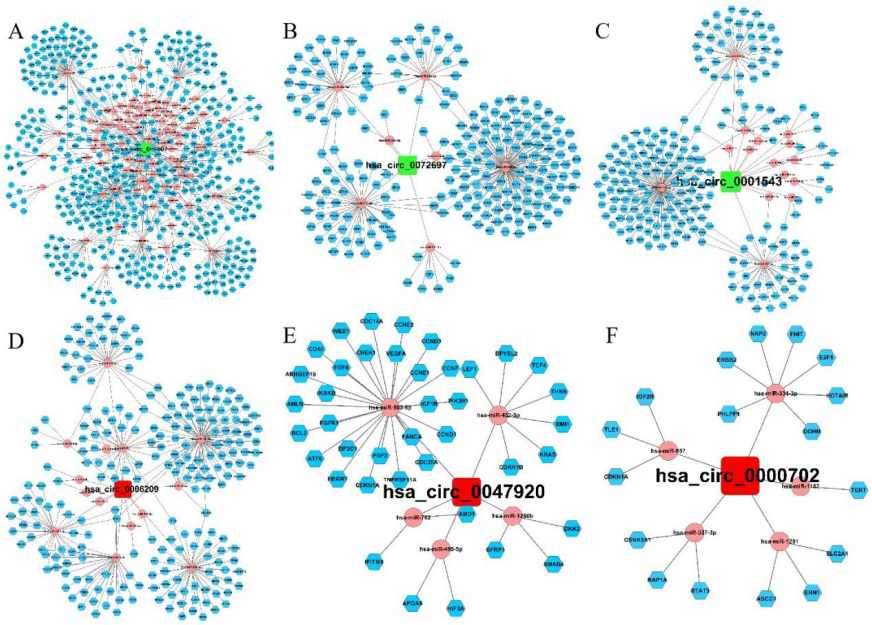

Figure 8. The sub circRNA-miRNA-mRNA ceRNA network.

This network was based on expression profile results and was created by specialized software. Dysregulated circRNAs (green and red nodes) with the highest magnitude of change, were predicted to be functionally connected with their targeted miRNAs in the network. hsa_circ_0005076(A), hsa_circ_0072697(B), hsa_circ_-0001543(C), hsa_circ_0006209(D), hsa_circ_0047920(E), hsa_circ_0000702(F).

Regulatory mechanism of hsa_circ_0072697 in AS-PBMCs

To investigate the regulatory mechanism of hsa_circ_0072697 in PBMCs of AS patients, we performed overexpression and knockdown of hsa_circ_0072697 in PBMCs, and divided them into 5 groups: AS-PBMC, AS-PBMC+pcDNA3.1 hsa_circ_0072697-NC, AS-PBMC+pcDNA3.1 hsa_circ_0072697, AS-PBMC+siRNA-hsa_circ_0072697-NC, AS-PBMC+siRNA-hsa_circ_0072697. CCK-8 assay showed that the cell proliferation activity of the hsa_circ_0072697 overexpression group was significantly reduced compared to the other four groups, while the cell proliferation activity of the siRNA-hsa_circ_0072697 group was increased (Fig. 9A). These results suggest that hsa_circ_0072697 may play an inhibitory role in the pathogenesis of AS. Furthermore, apoptosis analysis by flow cytometry showed that the hsa_circ_0072697 overexpression group had the highest apoptosis rate, while the siRNA-hsa_circ_0072697 group had the lowest apoptosis rate (Fig. 9B). This indicates that hsa_circ_0072697 is also involved in regulating the apoptosis of PBMCs. Finally, from cell cycle analysis performed by flow cytometry, we observed that the hsa_circ_0072697 overexpression group had a decrease in the number of cells in the G1 phase and an increase in the number of cells in the S and G2 phases compared to the control group, while the siRNA-hsa_circ_0072697 group had completely opposite effects on the cell cycle of PBMCs (Fig. 9C). These findings indicate that hsa_circ_0072697 plays an important role in the cell cycle of PBMCs.

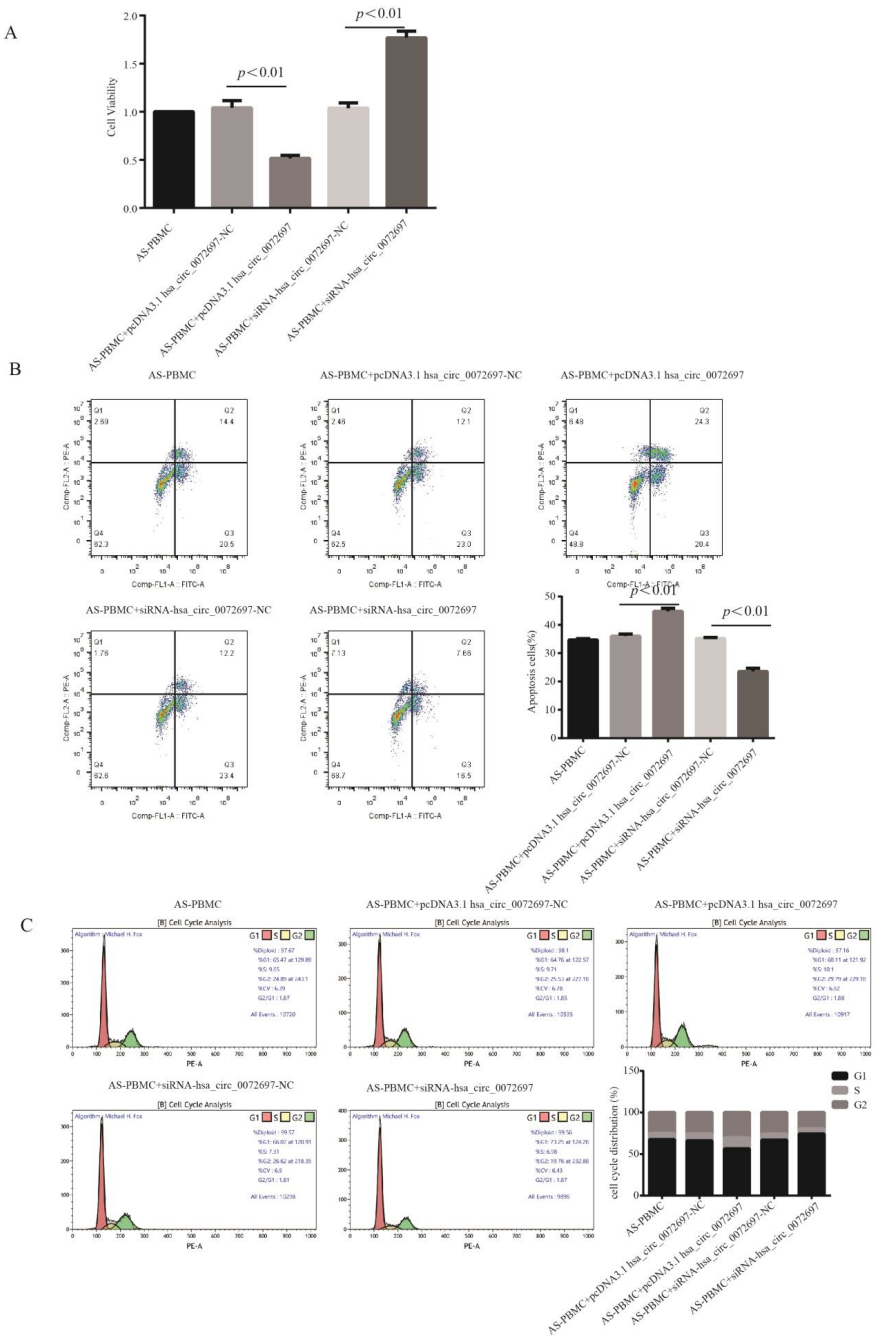

Figure 9. Effects of hsa_circ_0072697 overexpression and knockdown on PBMCs in AS patients.

(A) Cell proliferation activity of PBMCs in different groups measured by CCK-8 assay. The hsa_circ_-0072697 overexpression group showed significantly reduced cell proliferation activity compared to the other four groups, while the siRNA-hsa_circ_0072697 group showed increased cell proliferation activity.

(B) Apoptosis analysis of PBMCs in different groups by flow cytometry. The hsa_circ_0072697 overexpression group had the highest apoptosis rate, while the siRNA-hsa_circ_0072697 group had the lowest apoptosis rate.

(C) Cell cycle analysis of PBMCs in different groups by flow cytometry. The hsa_circ_0072697 overexpression

group showed a decrease in the number of cells in the G1 phase and an increase in the number of cells in the S and G2 phases compared to the control group, while the siRNA-hsa_circ_0072697 group showed completely opposite effects.

Impact of hsa_circ_0072697 expression levels on inflammatory cytokine concentrations in PBMCs of AS patients

Inflammatory cytokines, such as TNF-α, IL-4, IL-10, and IL-17, are involved in the pathogenesis of many inflammatory diseases, including AS(37-39). In this study, we investigated the effect of different expression levels of hsa_circ_0072697 on the concentration of inflammatory cytokines in PBMCs from AS patients using ELISA assay. As shown in Figure 10, the concentration of IL-4 and IL-10 was highest in the AS-PBMC+pcDNA3.1 hsa_circ_0072697 group, while the concentration of IL-17 and TNF-α was the lowest. In contrast, with the knockdown of hsa_circ_0072697 expression, the concentration of IL-17 and TNF-α increased, while the concentration of IL-4 and IL-10 significantly decreased. These results suggest that hsa_circ_0072697 may regulate the expression of inflammatory cytokines in AS, and targeting hsa_circ_0072697 may be a potential therapeutic strategy for AS treatment.

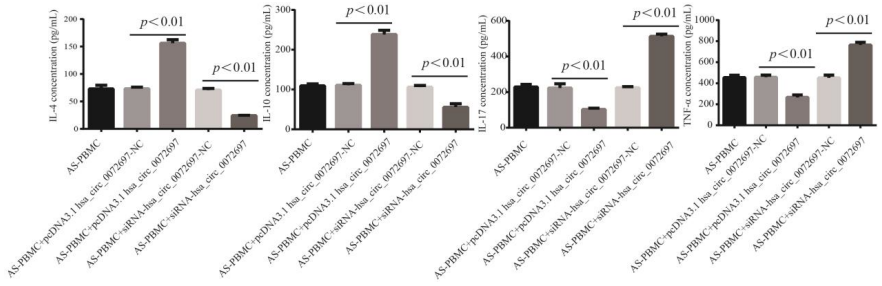

Figure 10. The effect of hsa_circ_0072697 on the expression of inflammatory factors in AS-PBMC.

Regulatory effects of hsa_circ_0072697 on AS-related factors in AS-PBMCs

We performed overexpression and knockdown of hsa_circ_0072697 in AS-PBMCs and evaluated the relative mRNA expression levels of hsa-miR-145-5p, MMP3, MMP9, IKB-α, and NF-κB p65 using RT-qPCR (Fig.11A). Our results demonstrated that the relative mRNA expression levels of hsa-miR-145-5p, MMP3, MMP9, and NF-κB p65 were downregulated in AS-PBMC+pcDNA3.1 hsa_circ_0072697 group and upregulated in AS-PBMC+siRNA-hsa_circ_0072697 group. Conversely, the expression of NF-κB p65 inhibitor IKB-α was upregulated in AS-PBMC+pcDNA3.1 hsa_circ_0072697 group and downregulated in AS-PBMC+siRNA-hsa_circ_0072697 group. Furthermore, WB assay showed that the protein levels of MMP3, MMP9, and p-NF-κB/NF-κB were reduced in AS-PBMC+pcDNA3.1 hsa_circ_0072697 group and increased in AS-PBMC+siRNA-hsa_circ_0072697 group. Meanwhile, the protein expression level of IKBα/p-IKBα was upregulated in AS-PBMC+pcDNA3.1 hsa_circ_0072697 group and downregulated in AS-PBMC+siRNA-hsa_circ_0072697 group (Fig.11B and 11C). These results indicated that the expression of hsa_circ_0072697 positively regulates IKBα/p-IKBα, and negatively regulates MMP3, MMP9, p-NF-κB/NF-κB.

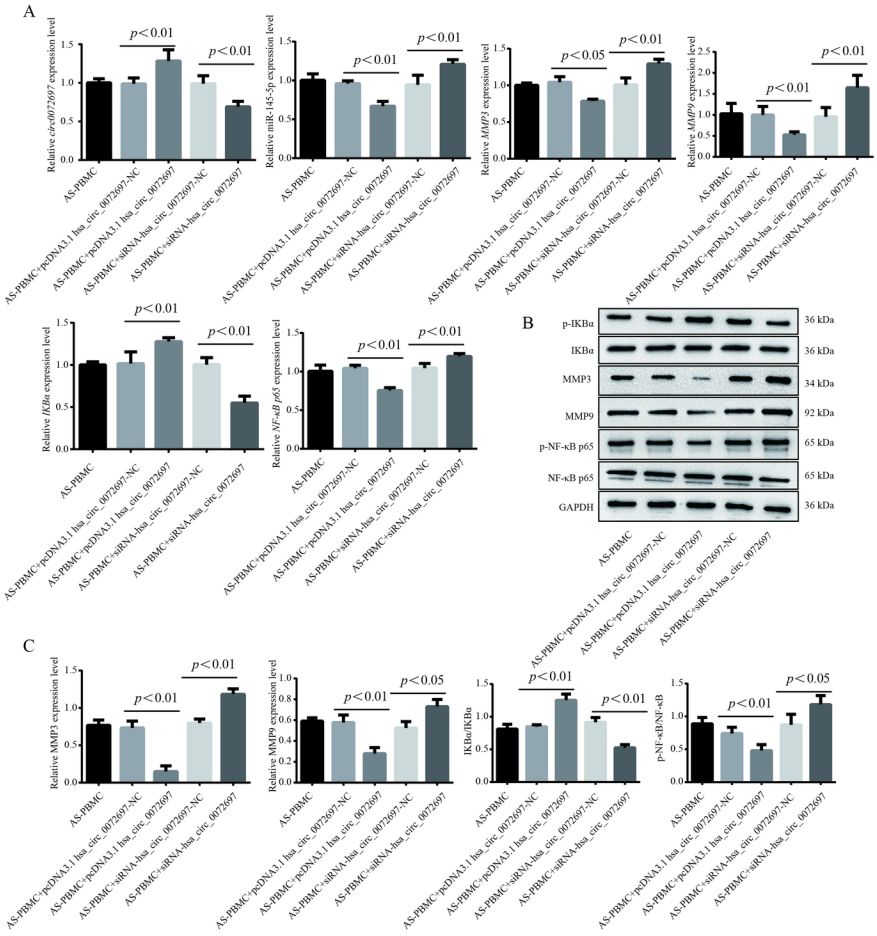

Figure 11 The effect of hsa_circ_0072697 on the related molecules in AS-PBMC .

(A) RT-qPCR analysis of relative mRNA expression levels of hsa-miR-145-5p, MMP3, MMP9, IKB-α, and NF-κB p65 in AS-PBMCs overexpressing or knocking down hsa_circ_0072697.

(B) and (C) Western blot analysis showing protein levels of MMP3, MMP9, p-NF-κB/NF-κB, IKBα/p-IKBα in AS-PBMCs in which hsa_circ_0072697 was overexpressed or knocked down.

ησα_cιρc_0072697 ρεγυλατες ΝΦ-κΒ πατηωαψ αcτιατιον βψ μοδυλατινγ π-ΝΦ-κΒ εξ-πρεσσιον ιν ΠΒΜ῾c οφ ΑΣ πατιεντ

In addition, we performed IF assays to investigate the expression of p-NF-κB and p-IKBα in PBMCs. As shown in Figure 12A, there was more green fluorescence in the AS-PBMC+pcDNA3.1 hsa_circ_0072697 group, indicating positive expression of p-IKBα in this group. However, Figure 12B showed that p-NF-κB was positively expressed (with a higher amount of green fluorescence) in the AS-PBMC+siRNA-hsa_circ_-0072697 group. These results suggest that hsa_circ_0072697 may regulate NF-κB pathway activation by modulating p-NF-κB expression.

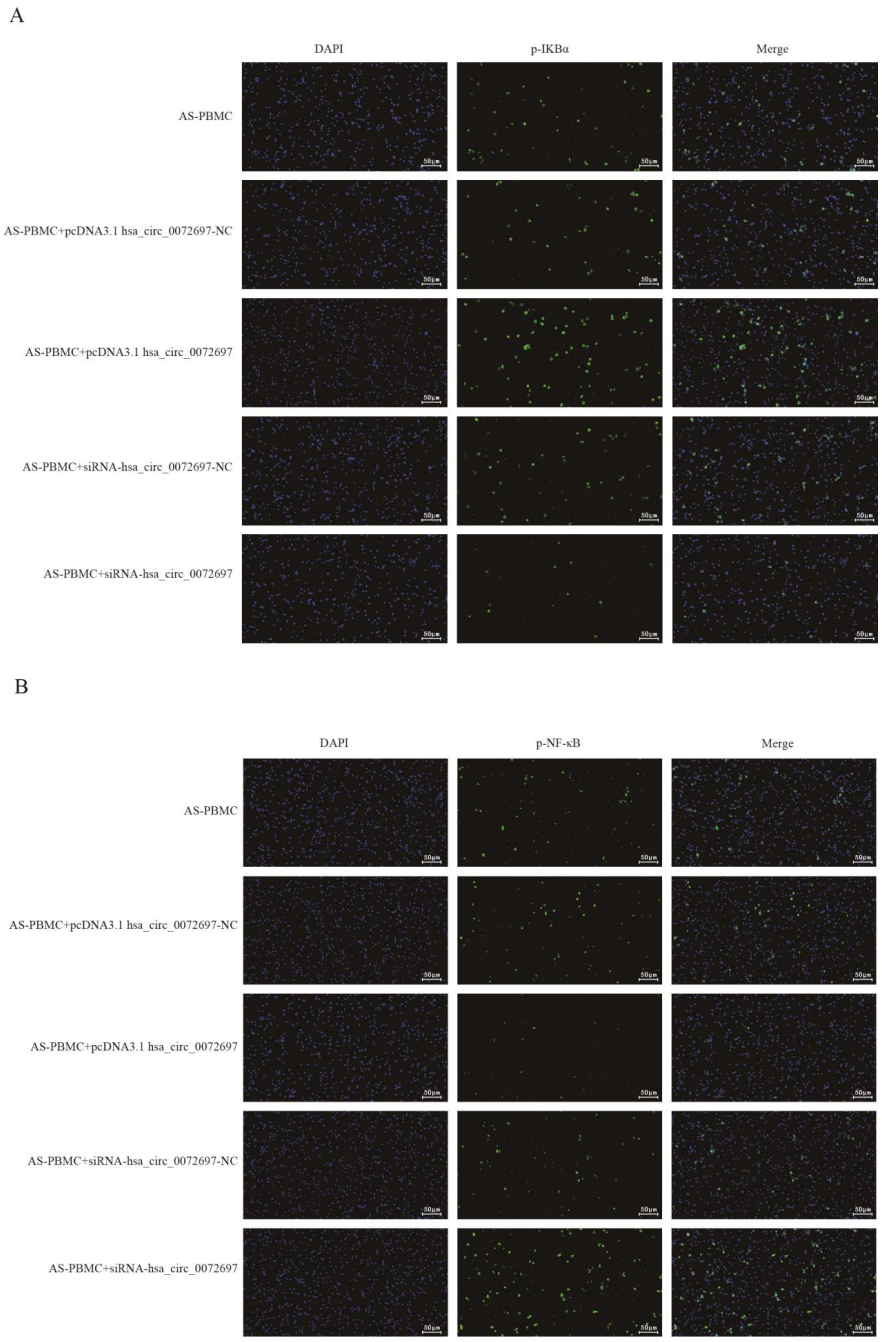

Φιγυρε 12. Ιμμυνοφλυορεσχενχε αναλψσις οφ π-ΝΦ-κΒ ανδ π-ΙΚΒα εξπρεσσιον ιν ΠΒΜ˜ς ωιτη διφφερεντ εξπρεσσιον λεελς οφ ησα_χιρς_0072697.

(A) Immunofluorescence assay of p-IKBα expression in AS-PBMCs overexpressing or knocking down hsa_circ_0072697. Green fluorescence indicates the positive expression of p-IKBα, and blue fluorescence indicates the nucleus.

(B) Immunofluorescence assay of p-NF-κB expression in AS-PBMCs overexpressing or knocking down hsa_circ_0072697. Green fluorescence indicates the positive expression of p-NF-κB, and blue fluorescence indicates

the nucleus.

Discussion

To date, tens of thousands of circRNAs have been reported in eukaryotic species, and their functional importance has attracted increasing interest in recent years[24, 25]. In a recent study, over 140,790 circRNAs were profiled in 20 clinically relevant tissues, revealing the tissue-specific expression patterns of some of these human circRNAs[26]. The sequestration of miRNAs via the sponge-like ceRNA mechanism is one of the best-characterized functional mechanisms by which circRNAs influence cell biology[26]. Some circRNAs possess numerous miRNA binding sites that enable them to effectively suppress miRNA functionality[30, 31]. Clear evidence has demonstrated roles for circRNAs in proliferation[32, 33], cell cycle progression[34], apoptosis[35, 36], and autophagy[37, 38].

In this study, we analyzed the expression of circRNA in PBMCs from AS patients and identified 131 DECs (89 upregulated and 42 downregulated) compared to DECs isolated from healthy controls. To verify the reliability of the sequencing data, three up-regulated (hsa_circ_0000702, hsa_circ_0006209, hsa_circ_0047920) and three down-regulated (hsa_circ_0001543, hsa_circ_0072697, hsa_circ_0005076) circRNAs were selected for RT-qPCR-based validation when analyzing a larger cohort of samples from AS and CN patients. KEGG analyses of the target genes associated with the six circRNAs with putative ceRNA functionality revealed these genes to be related to the p53, Adherens junction, ErbB, cell cycle, B cell receptor signaling, neurotrophin, Toll-like receptor, T cell receptor, VEGF, mTOR, focal adhesion, adipocytokine, Notch, NOD-like receptor, FceRI, and apoptotic signaling pathways. Further, correlation and ROC curve analyses revealed the expressions of hsa_circ_0006209 and hsa_circ_0047920 to be positively correlated with hs-CRP levels in AS patients, while hsa_circ_0072697 levels were positively correlated with ESR and BASDAI levels in this same patient cohort. ROC curve analysis demonstrated that hsa_circ_0072697 had the highest potential as a diagnostic biomarker for AS among the six validated circRNAs. Moreover, the ceRNA network constructed based on these circRNAs offers valuable insights into the regulatory mechanisms underlying AS and could be utilized to identify potential therapeutic targets. Recent studies have shown that hsa_ CircRNA_ 1012732 is correlated with indicators of AS disease activity, hsa_ CircRNA_ 1001544, hsa_ Circle_ 0000652 may be a molecular marker for diagnosing AS[39, 40].

As part of homeostasis, proliferation, inflammation, and apoptosis are highly regulated cellular processes[41]. Previous studies have shown that CircRNA is involved in various biological processes, including cell proliferation, apoptosis, invasion, and migration[42-45]. In the present study, in vitro cell experiments were used to thoroughly investigate the role of hsa_cir_0072697 in the pathogenesis of AS. It was found that overexpression of hsa_circ_0072697 inhibited PBMC proliferation and promoted apoptosis. Conversely, knockdown of hsa_circ_0072697 promoted PBMC proliferation and inhibited apoptosis. Additionally, hsa_circ_0072697 expression levels affected the cell cycle progression of PBMCs. We then analyzed the effect of hsa_circ_-0072697 expression on inflammatory cytokine expression (TNF-α, IL-4, IL-10, and IL-17) and key genes in the NF-kB pathway. Our results showed that overexpression of hsa_circ_0072697 increased IL-4 and IL-10 concentrations and decreased IL-17 and TNF-α concentrations. It also led to decreased expression of hsa-miR-145-5p, MMP3, MMP9, and NF-kB p65 mRNA, and increased expression of IKBα. Conversely, knockdown of hsa_circ_0072697 resulted in the opposite effects. Moreover, IF assays confirmed the effects of different hsa_circ_0072697 expression levels on p-IKBα and p-NF-ϰB. Our study highlights the importance of hsa_circ_0072697 in regulating the expression of key genes involved in the pathogenesis of AS, especially those involved in the NF-ϰB pathway. These findings shed new light on the molecular mechanisms underlying AS development and suggest potential therapeutic targets for the disease. However, further studies are needed to fully understand the underlying mechanism of hsa_circ_0072697 in AS pathogenesis and its potential as a therapeutic target.

Several limitations of this study should be acknowledged. Firstly, the sample size is relatively small, and larger studies with multi-ethnic populations are needed to validate and extend our findings. Secondly, we did not assess the ability of the identified circRNAs to differentiate AS patients from those with other autoimmune diseases, such as SLE, MS, or RA. Future studies should aim to evaluate the specificity of these

biomarkers by comparing their ability to distinguish AS from other related conditions.

In summary, we employ a high-throughput RNA-seq method in PBMCs samples to identify specific circRNA biomarkers that are specifically associated with the incidence of AS patients. The identified DECs and related ceRNA functions provide new directions for future research regarding the mechanistic basis for the pathogenesis of AS. Specially, we confirm that hsa_circ_0072697 has a good diagnostic value in AS patients, and it could suppress the progression of AS by targeting NF-$\varkappa$B pathway. These findings shed new lights on AS mechanism and clinical application in patients.

Supplementary Material

The datasets used for the current study are available from the corresponding author on reasonable request.

Acknowledgements

Not applicable.

Funding

This work was supported by the National Natural Science Foundation of China(82205054), Anhui Province Key Laboratory of Modern Chinese Medicine Department of Internal Medicine Application Foundation Research and Development (2021AKLMCM002), Key Project of Natural Science Foundation of Anhui Province for College Scholar (KJ2021A0558), Key laboratory opening project of the ministry of education of Xinan Medical Science (2020XAYX08), Construction project of Jian Liu studio of TCM in Anhui province (secretary of development of traditional Chinese medicine [2018] no. 11), The 12th batch of "115" innovation team in Anhui province (no. 1 [2019] of anhui talent office).

Authors Contribution

HD, LJ, and WY contributed to the study design. HD, FYY, and XD contributed to data analysis, wrote the first draft, and revised the manuscript. ZWD, WL and LY contributed to the specimen and date collection. LJ revised the manuscript critically for important intellectual content. All authors reviewed and accepted the content of the final manuscript.

Competing interests

The authors declare that they have no competing interests.

References:

[1] Shoenfeld Y, Selmi C, Zimlichman E, et al. The autoimmunologist: geoepidemiology, a new center of gravity, and prime time for autoimmunity. J Autoimmun. 2008, 31(4): 325-330.

[2] Wang F, Chu C, Zhao C, et al. Diffusion kurtosis imaging in sacroiliitis to evaluate the activity of ankylosing spondylitis. J Magn Reson Imaging: JMRI. 2019, 49(1).

[3] Ji W, Lu Y, Ma Z, et al. Triptolide attenuates inhibition of ankylosing spondylitis-derived mesenchymal stem cells on the osteoclastogenesis through modulating exosomal transfer of circ-0110634. J Orthop Translat. 2022, 36: 132-144.

[4] Xu F, Jin L, Jin Y, et al. Long noncoding RNAs in autoimmune diseases. J Biomed Mater Res A, 2019, 107: 468-475.

[5] Liu H, Zhu Z, Fang J, et al. The ceRNA Network Has Potential Prognostic Value in Clear Cell Renal Cell Carcinoma: A Study Based on TCGA Database. Biomed Res Int, 2020, 2020: 4830847.

[6] Chen L L, Yang L. Regulation of circRNA biogenesis. RNA Biol. 2015, 12(4): 381-388.

[7] Pamudurti N R, Bartok O, Jens M, et al. Translation of CircRNAs. Mol Cell. 2017, 66(1): 9-21.

[8] Zhong Y, Du Y, Yang X, et al. Circular RNAs function as ceRNAs to regulate and control human cancer progression. Mol Cancer. 2018, 17(1): 79.

[9] Wang J J, Shan K, Liu B H, et al. Targeting circular RNA-ZRANB1 for therapeutic intervention in retinal neurodegeneration. Cell Death Dis. 2018, 9(5): 540.

[10] Liu C, Zhang C, Yang J, et al. Screening circular RNA expression patterns following focal cerebral ischemia in mice. Oncotarget. 2017, 8(49): 86535-86547.

[11] Garlapati P, Ling J, Chiao P J, et al. Circular RNAs regulate cancer-related signaling pathways and serve as potential diagnostic biomarkers for human cancers. Cancer Cell Int. 2021, 21(1): 317.

[12] Han B, Zhang Y, Zhang Y, et al. Novel insight into circular RNA HECTD1 in astrocyte activation via autophagy by targeting MIR142-TIPARP: implications for cerebral ischemic stroke. Autophagy. 2018, 14(7): 1164-1184.

[13] Greene J, Baird A M, Brady L, et al. Circular RNAs: Biogenesis, Function and Role in Human Diseases. Front Mol Biosci. 2017, 4: 38.

[14] Li L J, Zhu Z W, Zhao W, et al. Circular RNA expression profile and potential function of hsa_circ_-0045272 in systemic lupus erythematosus. Immunology. 2018, 155(1): 137-149.

[15] Zhang C, Wang X, Chen Y, et al. The down-regulation of hsa_circ_0012919, the sponge for miR-125a-3p, contributes to DNA methylation of CD11a and CD70 in CD4(+) T cells of systemic lupus erythematous. Clin Sci (Lond). 2018, 132(21): 2285-2298.

[16] Iparraguirre L, Munoz-Culla M, Prada-Luengo I, et al. Circular RNA profiling reveals that circular RNAs from ANXA2 can be used as new biomarkers for multiple sclerosi. Hum Mol Genet. 2017, 26(18): 3564-3572.

[17] Zhong S, Ouyang Q, Zhu D, et al. Hsa_circ_0088036 promotes the proliferation and migration of fibroblast-like synoviocytes by sponging miR-140-3p and upregulating SIRT 1 expression in rheumatoid arthritis. Mol Immunol. 2020, 125: 131-139.

[18] Luo Q, Liu J, Fu B, et al. Circular RNAs Hsa_circ_0002715 and Hsa_circ_0035197 in Peripheral Blood Are Novel Potential Biomarkers for New-Onset Rheumatoid Arthritis. Dis Markers. 2019, 2019: 2073139.

[19] Zheng J, Li Z, Wang T, et al. Microarray Expression Profile of Circular RNAs in Plasma from Primary Biliary Cholangitis Patients. Cell Physiol Biochem. 2017, 44(4): 1271-1281.

[20] Li H, Yang H H, Sun Z G, et al. Whole-transcriptome sequencing of knee joint cartilage from osteoarthritis patients. Bone Joint Res. 2019, 8(7): 290-303.

[21] Li Z, Yuan B, Pei Z, et al. Circ_0136474 and MMP-13 suppressed cell proliferation by competitive binding to miR-127-5p in osteoarthritis. J Cell Mol Med. 2019, 23(10): 6554-6564.

[22] van der Linden S, Valkenburg H A, Cats A. Evaluation of diagnostic criteria for ankylosing spondylitis. A proposal for modification of the New York criteria. Arthritis Rheum. 1984, 27(4): 361-368.

[23] Acquaviva M, Menon R, Di Dario M, et al. Inferring Multiple Sclerosis Stages from the Blood Transcriptome via Machine Learning. Cell Rep Med. 2020, 1(4): 100053.

[24] Chen J, Yang X, Liu R, et al. Circular RNA GLIS2 promotes colorectal cancer cell motility via activation of the NF-kappaB pathway. Cell Death Dis. 2020, 11(9): 788.

[25] Li W, Yang P, Zhong C, et al. The circ-PITX1 promotes non-small cell lung cancer development via the miR-30e-5p/ITGA6 axis. Cell Cycle. 2022, 21(3): 304-321.

[26] Maass P G, Glazar P, Memczak S, et al. A map of human circular RNAs in clinically relevant tissues. J Mol Med (Berl). 2017, 95(11): 1179-1189.

[27] Ebbesen K K, Hansen T B, Kjems J. Insights into circular RNA biology. RNA Biol. 2017, 14(8): 1035-1045.

[28] Zhang M, Han Y, Zhai Y, et al. Integrative analysis of circRNAs, miRNAs, and mRNAs profiles to reveal ceRNAs networks in chicken intramuscular and abdominal adipogenesis. BMC Genomics. 2020, 21(1): 594.

[29] Zhu X, Wang X, Wang Y, et al. The regulatory network among CircHIPK3, LncGAS5, and miR-495 promotes Th2 differentiation in allergic rhinitis. Cell Death Dis. 2020, 11(4): 216.

[30] Wu H J, Zhang C Y, Zhang S, et al. Microarray Expression Profile of Circular RNAs in Heart Tissue of Mice with Myocardial Infarction-Induced Heart Failure. Cell Physiol Biochem. 2016, 39(1): 205-216.

[31] Shao Y, Song Y, Xu S, et al. Expression Profile of Circular RNAs in Oral Squamous Cell Carcinoma. Front Oncol. 2020, 10: 533616.

[32] Gao X, Ma X K, Li X, et al. Knockout of circRNAs by base editing back-splice sites of circularized exons. Genome Biol. 2022, 23(1): 16.

[33] Limb C, Liu D, Veno M T, et al. The Role of Circular RNAs in Pancreatic Ductal Adenocarcinoma and Biliary-Tract Cancers. Cancers (Basel). 2020, 12(11).

[34] Chen J, Chen T, Zhu Y, et al. circPTN sponges miR-145-5p/miR-330-5p to promote proliferation and stemness in glioma. J Exp Clin Cancer Res. 2019, 38(1): 398.

[35] Wang Z, Deng C, Zheng Y. Involvement of circRNAs in Proinflammatory Cytokines-Mediated beta-Cell Dysfunction. Mediators Inflamm. 2021, 2021: 5566453.

[36] Wang L, Wei Y, Yan Y, et al. CircDOCK1 suppresses cell apoptosis via inhibition of miR-196a-5p by targeting BIRC3 in OSCC. Oncol Rep. 2018, 39(3): 951-966.

[37] Song W, Zeng Z, Zhang Y, et al. CircRNF144B/miR-342-3p/FBXL11 axis reduced autophagy and promoted the progression of ovarian cancer by increasing the ubiquitination of Beclin-1. Cell Death Dis. 2022, 13(10): 857.

[38] Zhong C, Wu K, Wang S, et al. Autophagy-related circRNA evaluation reveals hsa_circ_0001747 as a potential favorable prognostic factor for biochemical recurrence in patients with prostate cancer. Cell Death Dis. 2021, 12(8): 726.

[39] Tang Y P, Zhang Q B, Dai F, et al. Circular RNAs in peripheral blood mononuclear cells from ankylosing spondylitis. Chin Med J (Engl). 2021, 134(21): 2573-2582.

[40] Song M, Gao J, Yan T, et al. Hsa_circ_0000652 Aggravates Inflammation by Activation of Macrophages and Enhancement of OX40/OX40L Interaction in Ankylosing Spondylitis. Front Cell Dev Biol. 2021, 9: 737599.

[41] Talbott S J, Luanpitpong S, Stehlik C, et al. S-nitrosylation of FLICE inhibitory protein determines its interaction with RIP1 and activation of NF-kappaB. Cell Cycle. 2014, 13(12): 1948-1957.

[42] Xu P, Zhang X, Cao J, et al. The novel role of circular RNA ST3GAL6 on blocking gastric cancer malignant behaviours through autophagy regulated by the FOXP2/MET/mTOR axis. Clin Transl Med. 2022, 12(1): e707.

[43] Xiang P, Ge T, Zhou J, et al. Protective role of circRNA CCND1 in ulcerative colitis via miR-142-5p/NCOA3 axis. BMC Gastroenterol. 2023, 23(1): 18.

[44] Cao J, Huang Z, Ou S, et al. circ0093740 Promotes Tumor Growth and Metastasis by Sponging miR-136/145 and Upregulating DNMT3A in Wilms Tumor. Front Oncol. 2021, 11: 647352.

[45] Wang F, Li J, Li L, et al. Circular RNA circ_IRAK3 contributes to tumor growth through upregulating KIF2A via adsorbing miR-603 in breast cancer. Cancer Cell Int. 2022, 22(1): 81.